

# Chapter 7

Unnatural Amino Acid Replacement Scanning  
in *Xenopus* oocytes

## 7.1 Introduction

There are many methodologies for the incorporation of unnatural amino acids (UAAs) *in vivo* (1–7). UAA incorporation by the endogenous translational machinery is typically performed in *E. coli* or other prokaryotes using auxotrophs (reassignment of sense codons) or by removing natural amino acids (aas) from growth media (statistical UAA incorporation) (8–19). Recent *in vitro* techniques identified 90 UAAs (59 previously unknown) that are substrates of *E. coli* aaRSs and aminoacylated onto tRNA (20). Of these 90, 71 UAAs were tested and 41 UAAs were accepted by the *E. coli* translational machinery *in vitro*, allowing for the simultaneous incorporation of 13 UAAs (21). UAA incorporation by the endogenous translational machinery in eukaryotic cells hasn't been studied extensively and experiments cause heterogeneous incorporation of UAAs (statistical UAA incorporation) in all proteins translated (22–24). Site-specific UAA incorporation, reassignment of sense codons, or statistical UAA incorporation is known to alter the stability, spectral properties, substrate binding, folding, expression, pore gating, and function of proteins (2–8,14,16,17,19,25–35).

Recently, UAAs have become commercially available for use in eukaryotic cells. Azidohomoalanine has been used to identify newly translated proteins in HEK cells and neurons (23) and is commercially available from Molecular Probes. Photoleucine (PLeu) and Photomethionine (PMet) (shown in Figure 7.1) are used to identify protein-protein interactions in eukaryotic cells (22) and are commercially available from Pierce. These UAAs are heterogeneously incorporated in all translated proteins upon supplementation in the growth media, but little is known about the effect (if any) on protein stability, folding, expression, and function.

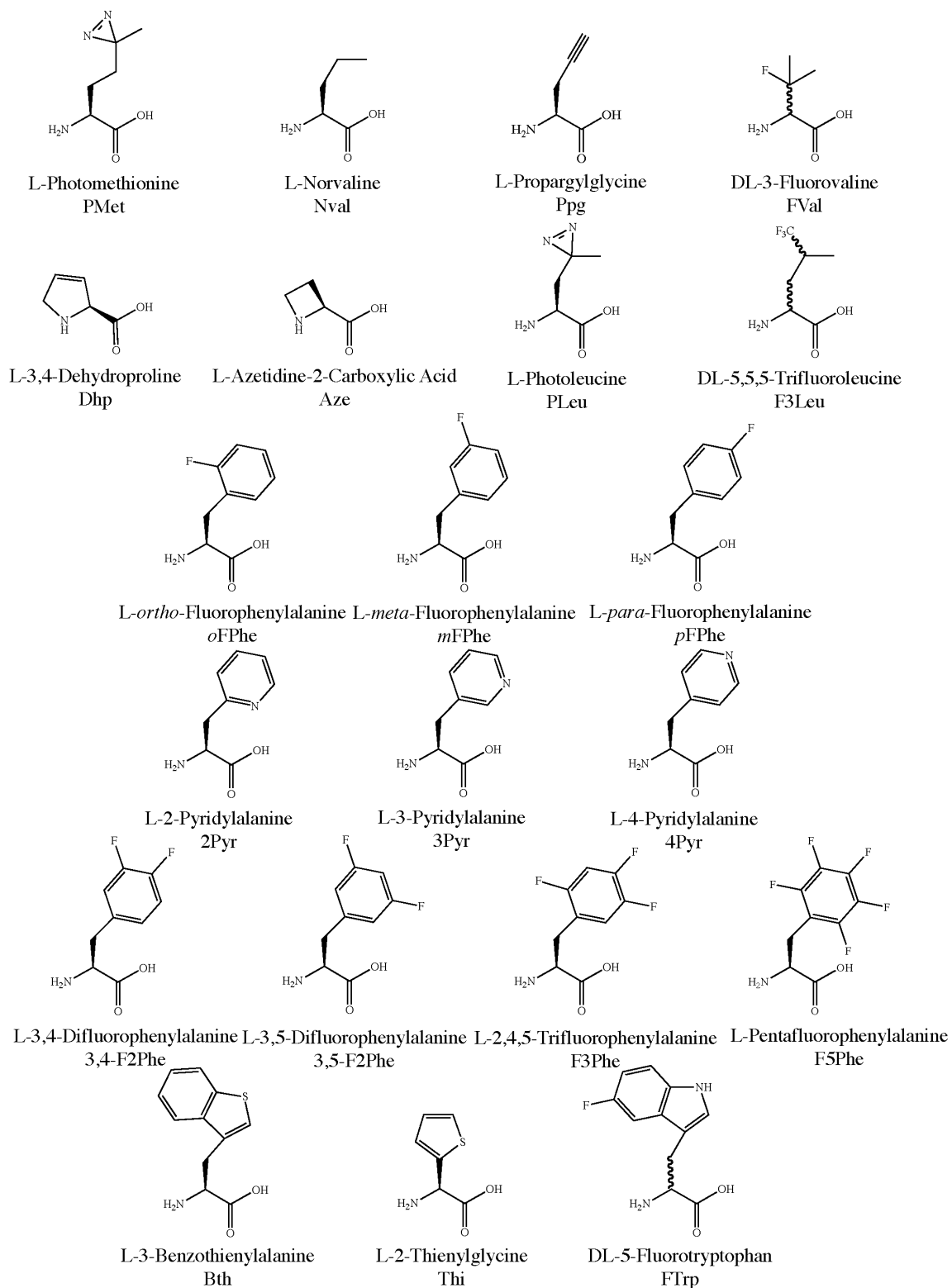


**Figure 7.1:** Unnatural amino acids used in this research.

In this research, we heterogeneously incorporated UAAs into the nicotinic acetylcholine receptor (nAChR) expressed in *Xenopus* oocytes. The heterogeneous incorporation of UAAs is termed unnatural amino acid replacement scanning (UAARS) because of the similarity to alanine scanning mutagenesis, where specific aas are mutated to Ala and the functions of proteins are examined. Because only UAAs that are similar to the cognate natural aa will be charged onto a tRNA, UAARS results in less side chain perturbation than most conventional mutagenesis. UAARS does not require DNA mutation and creates a large heterogeneous population of protein (discussed in detail below). The nAChR was expressed with UAAs in the incubation media, and changes in function were identified by shifts in  $EC_{50}$ . The incorporation of PLeu and PMet was also identified by inter-subunit cross-linking of the nAChR. The expression of functional ion channels on the surface of *Xenopus* oocytes was determined by electrophysiology and compared to total protein synthesized by Western blot analysis. UAARS should be useful for identifying UAAs that are recognized by the endogenous translational machinery, identifying changes in protein function without the need for DNA manipulation, and creation of extremely large populations of chemically unique proteins.

## 7.2 Results

### 7.2.1 Unnatural Amino Acid Replacement Scanning

In this research, the  $\alpha_{\text{HA His}}$  (contains the HA tag in the M3-M4 loop and a 6-His tag on the C-terminus) construct was initially used, because it was hoped that the  $\alpha$ -subunit could be purified using the 6-His tag as previously described (36). The  $EC_{50}$  of  $\alpha_{\text{HA His}}$  nAChR was reported as 25.5  $\mu\text{M}$  ACh (36), but references a paper that has a wild-

type nAChR  $EC_{50} = 47 \mu\text{M}$  (37). During the course of this research, the  $\alpha_{\text{HA His}}$  construct gave a variable  $EC_{50}$  ranging from 48–70  $\mu\text{M}$  depending on the batch of oocytes. The  $\alpha_{\text{NHA}}$  (contains the HA tag at the N-terminus) construct gave  $EC_{50}$  values ranging from 47–56  $\mu\text{M}$  and is a better construct for reproducible wild-type nAChR values. Due to the variability of the  $\alpha_{\text{HA His}}$   $EC_{50}$ , the UAARS experiments are compared to the  $\alpha_{\text{HA His}}$  wild-type  $EC_{50}$  recorded on the same batch of oocytes.

The *Xenopus* oocyte (stage VI) is a large cell measuring  $\approx 1.2\text{--}1.3$  mm in diameter (38,39). The oocyte starts at stage I and is approximately 0.1 mm in diameter (38). Oogenesis is asynchronous, and oocytes of all stages are present in the ovary of a *Xenopus laevis* frog (38). Complete oogenesis takes  $\sim 8$  months to reach stage VI, and oocytes remain in this stage until they are stimulated for maturation or the oocyte is absorbed by the ovary (38,39). During oogenesis, the oocyte accumulates ribosomes, yolk, glycogen, lipids, aas, and “maternal mRNA” (39). Oocytes contain a large pool of endogenous aas in preparation for protein synthesis (40). Heterologous expression of protein through injection of DNA or mRNA is an invaluable tool for studying ion channels, transporters, and receptors. Injected oocytes are typically incubated in saline solutions lacking any aas and still produce large amounts of protein (39,40).

Oocytes maintained in saline solution contain a large pool of aas that is greater than the concentration of aas found in *Xenopus laevis* plasma (40). The most abundant aas are Glu (3.6 mM) and Lys (1.1 mM), which are present in the plasma at concentrations of 0.11 mM and 0.29 mM, respectively (40). Oocytes maintained in saline solution have 0.20 mM Val, 0.19 mM Leu, and 0.13 mM Phe, but when incubated with saline solutions containing aas that mimic plasma concentrations, the oocytes uptake

aas to give 0.72 mM Val, 0.62 mM Leu, and 0.30 mM Phe (40). Therefore, oocytes rapidly import aas, and it was hoped that the same would occur for UAAs. The large endogenous pool of aas is a limiting factor for UAARS. Based on the determined concentration of aas in *Xenopus* oocytes kept in saline solution (40), Ile is the limiting aa, and yet there is enough Ile to make  $2.4 \times 10^{11}$  nAChRs (corresponding to  $6.1 \times 10^5$   $\mu$ A), which is at least three orders of magnitude greater expression than we ever see in a single oocyte. To incorporate UAAs by the endogenous translational machinery we must get a large amount of UAA inside the oocyte in order to compete with the endogenous aas.

Figure 7.2 schematically shows unnatural amino acid replacement scanning (UAARS) in *Xenopus* oocytes. Oocytes contain endogenous natural aas and are injected with mRNA for the nAChR. After injection, the oocytes are placed in media containing 0.5–4 mM UAA (Figure 7.2 A). The oocytes then begin to translate the nAChR, which depletes endogenous aas. Initially, all nAChRs are wild-type (containing no UAAs). Also during this time, UAAs are transported into the oocyte (Figure 7.2 B). Translation of the nAChR causes further depletion of the endogenous aas. As the concentration of UAA increases in the oocyte, an endogenous aminoacyl-tRNA synthetase (aaRS) recognizes the UAA and charges the cognate tRNA. The UAA is then heterogeneously incorporated into the nAChR at all positions recognized by the tRNA (Figure 7.2 C). Further incubation causes increased UAAs inside of the oocyte and further incorporation into the nAChR (Figure 7.2 D). During the incubation periods, the media is changed every 24 h to maintain excess UAA and to increase incorporation into the nAChR. After an incubation period, the oocytes are assayed by electrophysiology to determine shifts in  $EC_{50}$  and alterations in functional ion channel expression relative to oocytes not incubated

with UAAs. Electrophysiology only detects channels that are functional (gated by acetylcholine (ACh)) and on the oocyte membrane surface. For the UAAs PLeu and PMet (shown in Figure 7.1), oocytes were irradiated with UV to cross-link the subunits within an individual nAChR and analyzed by Western blot for increased molecular weight bands. Oocytes can also be analyzed by whole-cell Western blot to determine the total amount of protein translated (nAChR that is on the membrane surface, in the endoplasmic reticulum, in the golgi apparatus, and in vesicles) relative to oocytes not incubated with UAAs.

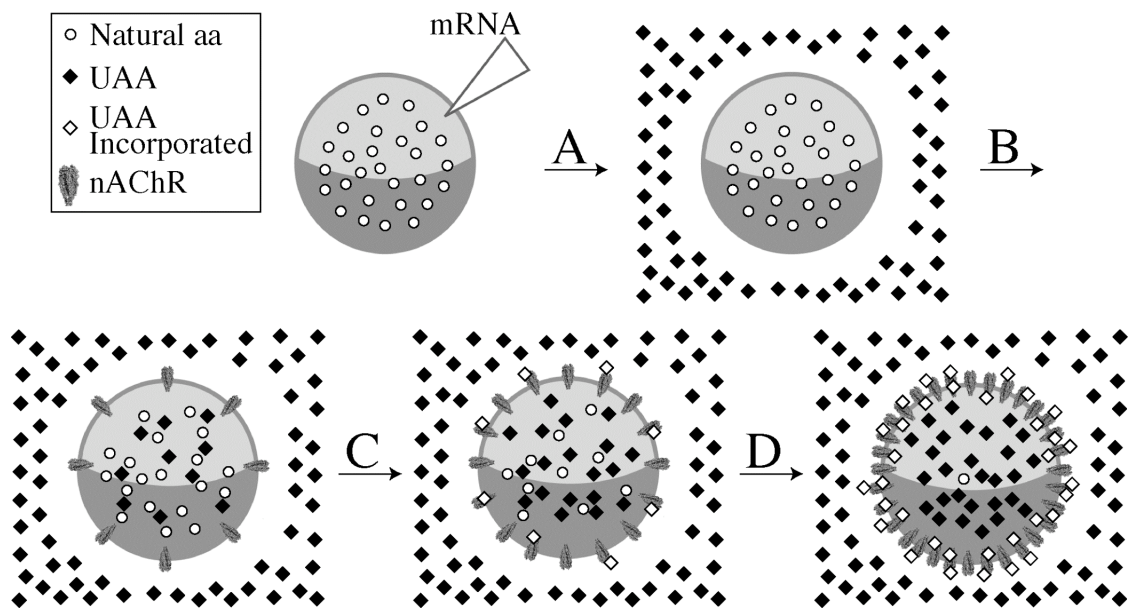


**Figure 7.2:** Unnatural amino acid replacement scanning (UAARS). A) Oocytes are injected with wild-type nAChR mRNA, which have endogenous, natural aas. The oocytes are placed in media containing UAAs and lacking the natural aa. B) After incubation; mRNA is translated, endogenous aas are depleted, and UAAs are transported inside the oocyte. C) With further incubation; more mRNA is translated, endogenous aas are further depleted, more UAAs are transported inside the oocyte, and UAAs are heterogeneously incorporated into the nAChR. D) Increased incubation time causes further mRNA translation, depletion of endogenous aas, increased UAAs inside the oocyte, and increased heterogeneous incorporation of UAAs into the nAChR. Figure adapted from (4) and nAChR created from 2BG9.pdb (41).

UAARS creates a large population of nAChRs, which is unprecedented without mutating DNA. For example, there are 251 Leu residues in the mouse muscle nAChR, and this is the most abundant aa (Figure 7.3). There are 37 Leu in the  $\alpha$ -subunit, 57 Leu in the  $\beta$ -subunit, 65 Leu in the  $\gamma$ -subunit, and 55 Leu in the  $\delta$ -subunit. The subunit stoichiometry of the nAChR is  $2\alpha:\beta:\gamma:\delta$  (Figure 6.1). Treating each of the five subunits as chemically distinct, there are 251 possible nAChRs when only a single UAA is incorporated. If a single UAA is incorporated in three of the subunits, there are  $1.2 \times 10^6$  possible nAChRs. A single UAA incorporated in each of the five subunits results in  $2.8 \times 10^8$  possible nAChRs. If all of the 251 sites can contain either Leu or an UAA, there are  $7.8 \times 10^{16}$  possible nAChRs, which is  $7.8 \times 10^5$  times greater than the  $\sim 1 \times 10^{11}$  neurons in an adult human brain. This example only includes UAARS at Leu but in theory incorporation at multiple UAAs is possible and can create increased populations of nAChRs.

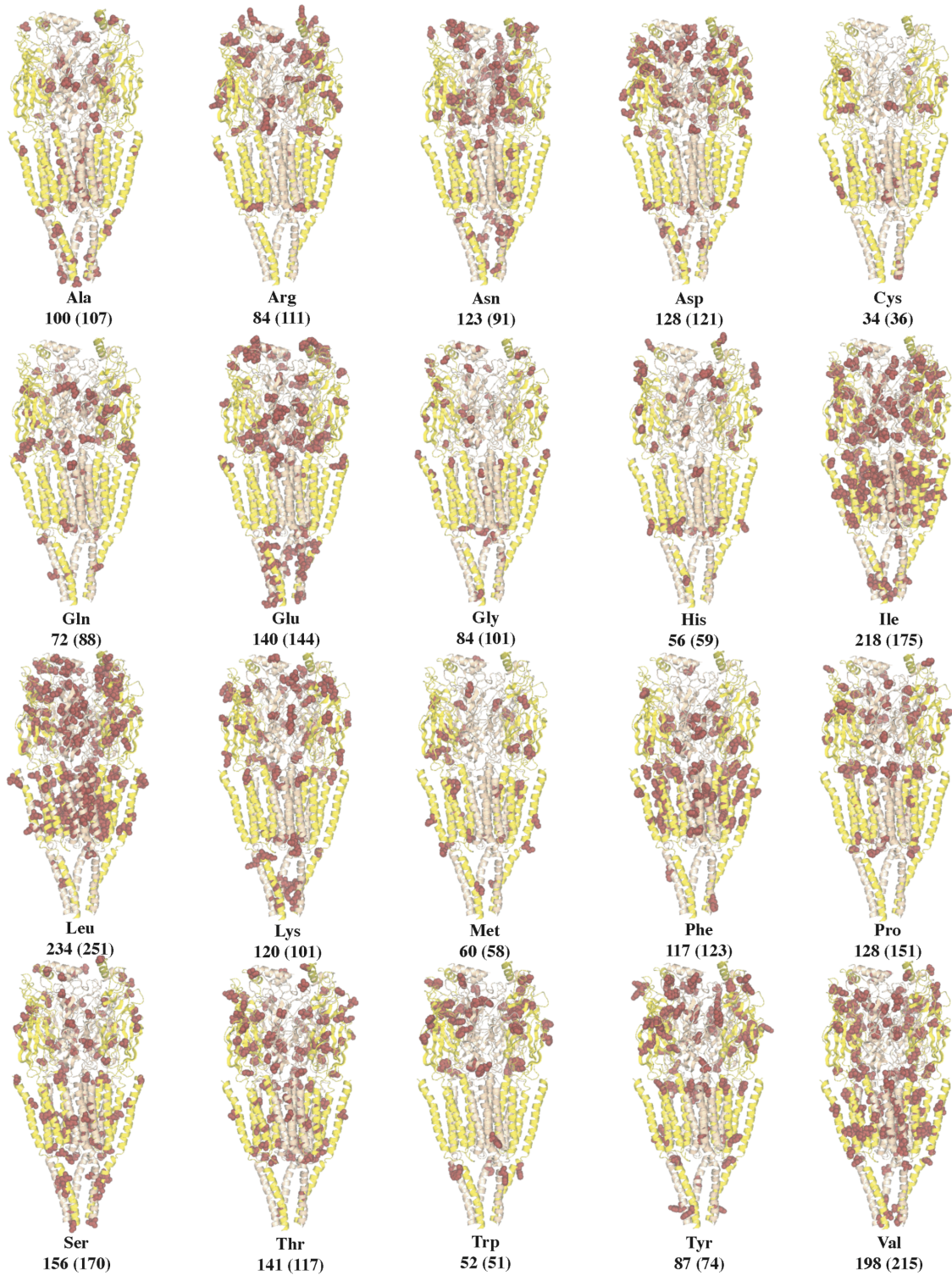


**Figure 7.3:** Amino acid composition of the nAChR. Number on left is the number of aas in the *Torpedo* nAChR (shown in red) and (number) is the number of aas in the mouse muscle nAChR. The  $\alpha$ -subunit is shown in yellow and all other subunits are beige. Images created from 2BG9.pdb (41).

### 7.2.2 Met Derivatives

There are 58 Met aas in the nAChR (Figure 7.3). PMet (shown in Figure 7.1) is accepted by the translational machinery and incorporated into proteins in COS7 (monkey kidney) and HeLa (human cervical cancer) cells (22). UAARS with PMet showed no significant shift in  $EC_{50}$  (Table 7.1). Nval (shown in Figure 7.1) is accepted by the *E. coli* methionyl-aminoacyl synthetase (MetRS) and aminoacylated on tRNA<sup>Met</sup> *in vitro* (20), and Nval is also accepted by the *E. coli* translational machinery *in vitro* (21). Nval incorporation was also detected in *E. coli* Met auxotrophs *in vivo* (13). UAARS with Nval showed no significant shift in  $EC_{50}$  (Table 7.1). Ppg has been shown to be accepted by the *E. coli* MetRS and aminoacylated on tRNA<sup>Met</sup> *in vitro* (20), but was not accepted by the *E. coli* translational machinery *in vitro* and *in vivo* (13,21). UAARS with Ppg showed no shift in  $EC_{50}$  (Table 7.1). While no significant shift was seen in the  $EC_{50}$  for these three Met derivatives, UAA incorporation into the nAChR may occur and cause no change in function. Other methods may be necessary for detection or UAARS into other ion channels.

**Table 7.1:** UAARS EC<sub>50</sub> determination

	UAA	EC <sub>50</sub>	Shift <sup>a</sup>	n <sub>H</sub>	n <sup>b</sup>	Incubation	
						Time	[UAA] <sup>c</sup>
<b>Met Derivatives</b>	PMet	64 ± 1	1.05	1.5 ± .04	8	48 h	0.5 mM
	Nval	49 ± 1	1.02	1.5 ± 1	7	48 h	1 mM
	Ppg	72 ± 4	1.07	1.5 ± .09	8	48 h	2 mM
<b>Pro Derivatives</b>	Dhp	58 ± 3	1.16	1.4 ± .08	6	48 h	1 mM
	Dhp	39 ± 2	1.33	1.5 ± .07	5	120 h	4 mM
	Aze	48 ± 1	1.04	1.4 ± .05	8	48 h	1 mM
	Aze	38 ± 1	1.37	1.4 ± .08	7	120 h	4 mM
<b>Val Derivative</b>	FVal	81 ± 3	1.65	1.7 ± .09	7	48 h	2 mM
<b>Leu Derivatives</b>	PLeu	18 ± 2	3.72	.93 ± .07	6	48 h	0.5 mM
	PLeu	17 ± 2	3.94	.99 ± .1	4	48 h	1 mM
	PLeu	2.5 ± .3	21.2	1.1 ± .1	6	120 h	1 mM
	F3Leu	25 ± 1	2.12	1.1 ± .05	6	48 h	2 mM
	F3Leu	11 ± 1	4.82	1.2 ± .1	7	120 h	2 mM
<b>Phe Derivatives</b>	<i>o</i> FPhE	82 ± 3	1.57	1.4 ± .06	6	48 h	1 mM
	<i>m</i> FPhE	32 ± 1	1.66	1.1 ± .06	7	48 h	1 mM
	<i>p</i> FPhE	8.2 ± .4	6.46	0.89 ± .03	6	48 h	1 mM
	3,4-F2PhE	53 ± 0.8	1.26	1.2 ± .01	8	48 h	2 mM
	3,5-F2PhE	69 ± 1	1.03	1.4 ± .03	8	48 h	2 mM
	F3PhE	60 ± 2	1.12	1.5 ± .05	8	48 h	2 mM
	F5PhE	63 ± 0.9	1.06	1.6 ± .03	8	48 h	2 mM
	2Pyr	74 ± 1	1.35	1.3 ± .02	6	48 h	2 mM
	3Pyr	41 ± .9	1.22	1.5 ± .04	5	48 h	2 mM
	4Pyr	51 ± 1	1.08	1.4 ± .05	5	48 h	2 mM
<b>Trp Derivatives</b>	Bth	49 ± 1	1.1	1.4 ± .05	6	48 h	2 mM
	Thi	52 ± 2	1.06	1.2 ± .05	6	48 h	2 mM
	FTrp	144 ± 9	2.88	1.4 ± .09	7	48 h	2 mM
<b>Multiple UAAs</b>	PMet + PLeu	13 ± 2	5.08	1.4 ± .2	6	48 h	0.5 mM PMet 1 mM PLeu

<sup>a</sup> Shift in EC<sub>50</sub> relative to wild-type nAChR EC<sub>50</sub> recorded on the same day.

<sup>b</sup> Number of oocytes.

<sup>c</sup> Concentration of UAA in media.

### 7.2.3 Pro Derivatives

There are 151 Pro aas in the nAChR (Figure 7.3). Dhp (shown in Figure 7.1) is recognized by the *E. coli* prolyl-aminoacyl tRNA synthetase (ProRS) *in vitro* (20) and accepted by the *E. coli* translational machinery *in vitro* (21). Dhp has also been

incorporated into protein expressed in *E. coli* (10). UAARS with Dhp shows only a slight shift in  $EC_{50}$  with a 2 d incubation (Table 7.1). UAARS with Dhp shows a meaningfully increased shift in  $EC_{50}$  with a 5 d incubation (Table 7.1). Aze (shown in Figure 7.1) is recognized by the *E. coli* ProRS *in vitro* (20) and accepted by the *E. coli* translational machinery *in vitro* (21). Aze has also been incorporated into protein expressed in *E. coli* (9). UAARS with Aze shows no shift in  $EC_{50}$  with a 2 d incubation (Table 7.1). With a 5 d incubation, Aze shows a significant shift in  $EC_{50}$  (Table 7.1). Both Dhp and Aze show significant shifts in  $EC_{50}$  that are gain of function (GOF) phenotypes with 5 d incubations, but are insignificant with 2 d incubations. Further incubation time may be necessary to obtain more efficient incorporation of these Pro derivatives.

#### **7.2.4 Val Derivative**

There are 215 Val aas in the nAChR (Figure 7.3). FVal (shown in Figure 7.1) is recognized by the *E. coli* valyl-aminoacyl tRNA synthetase *in vitro* (20) and accepted by the *E. coli* translational machinery *in vitro* (21). UAARS with FVal shows a significant 1.7-fold shift in  $EC_{50}$  (Table 7.1) and causes a loss of function (LOF) phenotype.

#### **7.2.5 Leu Derivatives**

There are 251 Leu aas in the nAChR, which is the most abundant aa (Figure 7.3). PLeu is accepted by the translational machinery and incorporated into proteins in COS7 and HeLa cells (22). UAARS shows a 3.7- and 3.9-fold shift in  $EC_{50}$  with 0.5 mM and 1 mM PLeu, respectively (Figure 7.4 A). This experiment clearly illustrates that 0.5 mM PLeu in the media is sufficient and gives approximately the same  $EC_{50}$  as 1 mM PLeu. UAARS shows no shift in  $EC_{50}$  with 0.5 mM and 1 mM PMet (Figure 7.4 A). *In vivo*

cross-linking experiments typically use both PLeu and PMet (22). UAARS with PLeu and PMet show 5.1-fold shift in  $EC_{50}$  (Figure 7.4 A). This  $EC_{50}$  is approximately the same for PLeu incorporation alone (Figure 7.4 A), showing that changes in nAChR function is primarily, if not exclusively, due to PLeu incorporation alone.

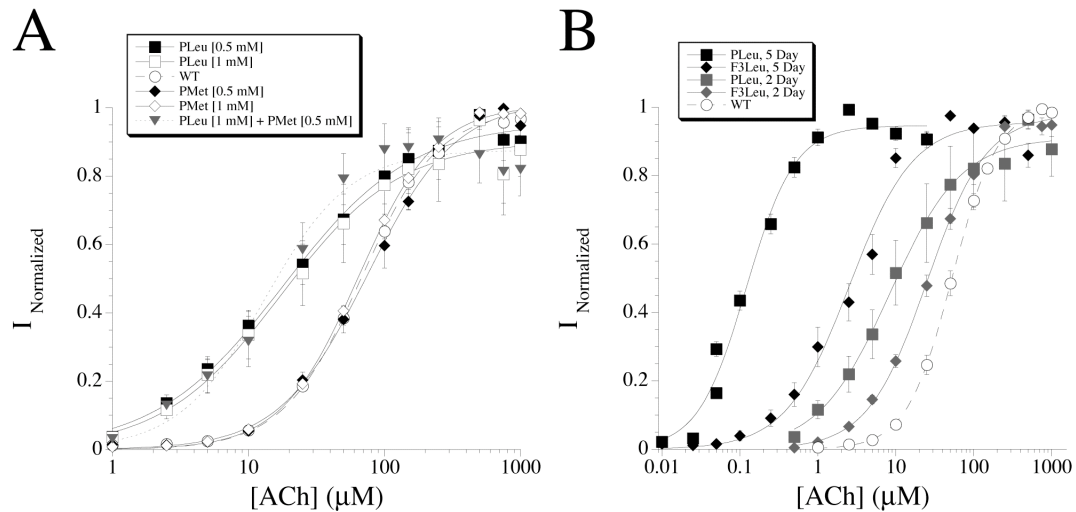


**Figure 7.4:** Fits to the Hill equation for UAARS with PLeu, PMet, and F3Leu. A) UAARS with PLeu, PMet, and PLeu + PMet. PLeu [0.5 mM]  $EC_{50} = 18 \pm 2$  and  $n_H = 0.93 \pm 0.07$ . PLeu [1 mM]  $EC_{50} = 17 \pm 2$  and  $n_H = 0.99 \pm 0.1$ . Wild-type  $\alpha_{HA His}$  nAChR  $EC_{50} = 67 \pm 2$  and  $n_H = 1.5 \pm 0.06$ . PMet [0.5 mM]  $EC_{50} = 75 \pm 4$  and  $n_H = 1.4 \pm 0.09$ . PMet [1 mM]  $EC_{50} = 64 \pm 1$  and  $n_H = 1.5 \pm 0.04$ . PLeu [1 mM] + PMet [0.5 mM]  $EC_{50} = 13 \pm 2$  and  $n_H = 1.4 \pm 0.2$ . In each experiment  $n > 4$  oocytes. B) UAARS with PLeu and F3Leu with 2 and 5 d incubations. PLeu (5 d incubation)  $EC_{50} = 2.5 \pm 0.3$  and  $n_H = 1.1 \pm 0.1$ . F3Leu (5 d incubation)  $EC_{50} = 11 \pm 1$  and  $n_H = 1.2 \pm 0.1$ . PLeu (2 d incubation)  $EC_{50} = 17 \pm 2$  and  $n_H = 0.99 \pm 0.1$ . F3Leu (2 d incubation)  $EC_{50} = 25 \pm 1$  and  $n_H = 1.1 \pm 0.05$ . Wild-type  $\alpha_{HA His}$  nAChR  $EC_{50} = 53 \pm 0.7$  and  $n_H = 1.5 \pm 0.02$ . In each experiment  $n > 3$  oocytes.

F3Leu (shown in Figure 7.1) is recognized by the *E. coli* leucyl-aminoacyl tRNA synthetase *in vitro* (20) and accepted by the *E. coli* translational machinery *in vitro* (21). F3Leu has also been incorporated in proteins expressed in *E. coli* auxotrophs *in vivo* (17). UAARS with F3Leu shows a 2.1- and 4.8-fold shift in  $EC_{50}$  with 2 and 5 d incubation, respectively (Figure 7.4 B). UAARS with PLeu shows a 3.9- and 21-fold shift in  $EC_{50}$

with 2 and 5 d incubation, respectively (Figure 7.4 B). Both F3Leu and PLeu show increased UAA incorporation with increased time, but the shift in F3Leu (2.3 from 5 d to 2 d) is not as strong as PLeu (5.4 from 5 d to 2 d) even though these UAAs are both replacing Leu.

### 7.2.6 Phe Derivatives

There are 123 Phe aas in the nAChR (Figure 7.3). *o*FPhe is recognized by the *E. coli* phenylalanyl-aminoacyl tRNA synthetase (PheRS) *in vitro* (20) and accepted by the *E. coli* translational machinery *in vitro* (21). *o*FPhe, *m*FPhe, and *p*FPhe have been incorporated into proteins expressed in *P. aeruginosa* (16). *p*FPhe has also been incorporated in proteins expressed in *E. coli* auxotrophs *in vivo* (8). UAARS with *o*FPhe shows a 1.6-fold shift in EC<sub>50</sub> and causes a LOF phenotype (Figure 7.5 A). UAARS with *m*FPhe shows a 1.7-fold shift in EC<sub>50</sub> and causes a GOF phenotype (Figure 7.5 A). UAARS with *p*FPhe shows a 6.5-fold shift in EC<sub>50</sub>, causes a GOF phenotype, and causes the largest shift with a 2 d incubation of all the UAAs shown in Figure 7.1. The shifts for *o*FPhe, *m*FPhe, and *p*FPhe were observed for two different batches of oocytes. UAARS with *o*FPhe, *m*FPhe, and *p*FPhe shows that the nAChR functions differently when the fluorine substituent is moved around the phenyl ring.

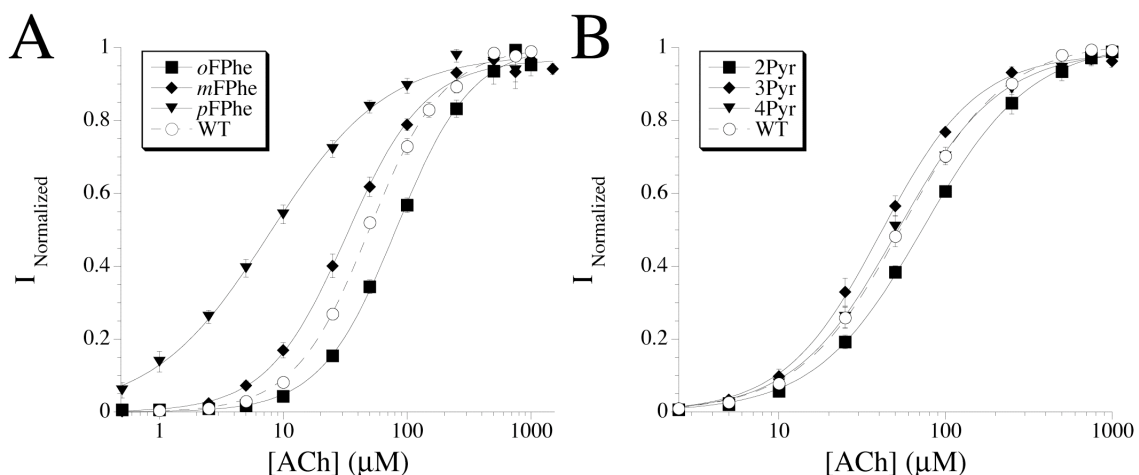


**Figure 7.5:** Fits to the Hill equation for UAARS with *o*FPhe, *m*FPhe, *p*FPhe, 2Pyr, 3Pyr, and 4Pyr. A) UAARS with *o*FPhe, *m*FPhe, and *p*FPhe. *o*FPhe  $EC_{50} = 82 \pm 3$  and  $n_H = 1.4 \pm 0.06$ . *m*FPhe  $EC_{50} = 32 \pm 1$  and  $n_H = 1.1 \pm 0.06$ . *p*FPhe  $EC_{50} = 8.2 \pm 0.4$  and  $n_H = 0.89 \pm 0.03$ . Wild-type  $\alpha_{HA} His$  nAChR  $EC_{50} = 49 \pm 1$  and  $n_H = 1.4 \pm 0.04$ . In each experiment  $n > 5$  oocytes. A) UAARS with 2Pyr, 3Pyr, and 4Pyr. 2Pyr  $EC_{50} = 74 \pm 1$  and  $n_H = 1.3 \pm 0.02$ . 3Pyr  $EC_{50} = 41 \pm 0.9$  and  $n_H = 1.5 \pm 0.04$ . 4Pyr  $EC_{50} = 51 \pm 1$  and  $n_H = 1.4 \pm 0.05$ . Wild-type  $\alpha_{NHA}$  nAChR  $EC_{50} = 55 \pm 0.9$  and  $n_H = 1.4 \pm 0.03$ . In each experiment  $n > 4$  oocytes.

2Pyr, 3Pyr, and 4Pyr (shown in Figure 7.1) have been incorporated in proteins expressed in *E. coli* auxotrophs *in vivo* (15,18). UAARS with 2Pyr shows a 1.4-fold shift in  $EC_{50}$  and causes a LOF phenotype (Figure 7.5 B). UAARS with 3Pyr shows a 1.2-fold shift in  $EC_{50}$  and causes a GOF phenotype (Figure 7.5 B). Both 2Pyr and 3Pyr show a similar phenotypical shift in  $EC_{50}$  to *o*FPhe and *m*FPhe, respectively (Figure 7.5 A & B). UAARS with 4Pyr shows no shift in  $EC_{50}$  (Figure 7.5). The lack of  $EC_{50}$  shift for 4Pyr suggests that or the loss of hydrogen at the *para* position has no affect on nAChR function. Overall, the pyridylalanine UAAs show smaller shifts in  $EC_{50}$  when compared to the fluorinated Phe UAAs.

UAARS with 3,4-F2Phe (shown in Figure 7.1) showed only a slight 1.3-fold shift in  $EC_{50}$  (Table 7.1) and further incubation time may be necessary to get increased UAA incorporation. UAARS with 3,5-F2Phe, F3Phe, and F5Phe (shown in Figure 7.1) all

showed slight shifts in  $EC_{50}$  (Table 7.1). F5Phe has been shown not to be accepted by the *E. coli* PheRS and a mutant *E. coli* PheRS *in vivo* (15). It appears that the addition of further fluorine substituents on the phenyl ring appears to block recognition by the *Xenopus* PheRS.

### 7.2.7 Trp Derivatives

There are 51 Trp aas in the nAChR (Figure 7.3). Bth and Thi (shown in Figure 7.1) are recognized by the *E. coli* tryptophanyl-aminoacyl tRNA synthetase (TrpRS) *in vitro* (20) and accepted by the *E. coli* translational machinery *in vitro* (21). Bth and Thi are both thought to be non-coding or not accepted *in vivo* (6). UAARS with Bth and Thi show no shift in  $EC_{50}$  (Table 7.1). Bth and Thi may be incorporated in the nAChR, but other methodologies for detection may be necessary.

FTrp is recognized by the *E. coli* TrpRS *in vitro* (20) and accepted by the *E. coli* translational machinery *in vitro* (21). FTrp is incorporated into proteins in *E. coli* (19). UAARS with FTrp results in a 2.9-fold shift in  $EC_{50}$  (Figure 7.6 A), and FTrp shows the greatest LOF phenotype of the UAAs tested in Figure 7.1. The UAARS with FTrp  $EC_{50}$  is close to the  $EC_{50}$  of the site-specific incorporation of FTrp at  $\alpha 149$  (Figure 7.6 A), which makes a cation- $\pi$  interaction with ACh (30).

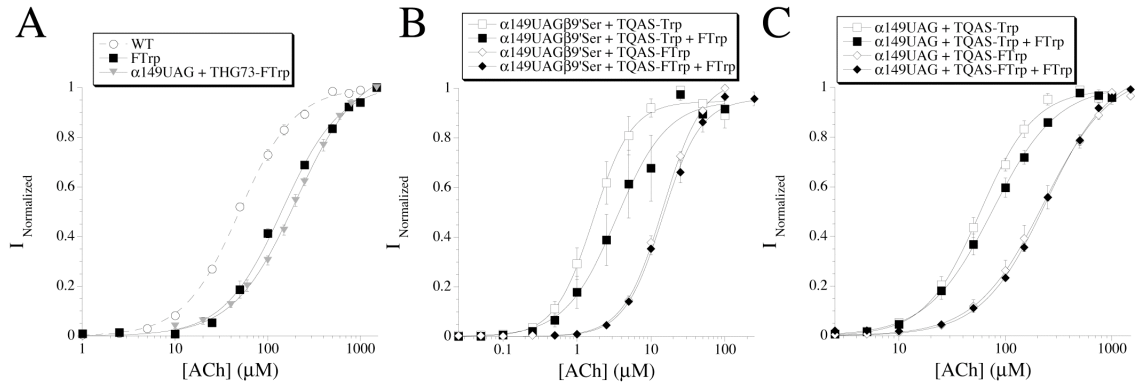


**Figure 7.6:** Fits to the Hill equation for UAARS with FTrp and nonsense suppression experiments. A) UAARS with FTrp. Wild-type  $\alpha_{\text{NHA}}$  nAChR  $EC_{50} = 48 \pm 2$  and  $n_H = 1.5 \pm 0.03$ . FTrp  $EC_{50} = 140 \pm 9$  and  $n_H = 1.4 \pm 0.09$ .  $\alpha 149\text{UAG} + \text{THG73-FTrp}$   $EC_{50} = 200 \pm 7$  and  $n_H = 1.3 \pm 0.04$ . In each experiment  $n > 5$  oocytes. B)  $\alpha 149\text{UAG}\beta 9'\text{Ser}$  nonsense suppression and UAARS with FTrp.  $\alpha 149\text{UAG}\beta 9'\text{Ser} + \text{TQAS-Trp}$   $EC_{50} = 1.7 \pm 0.1$  and  $n_H = 1.7 \pm 0.1$ .  $\alpha 149\text{UAG}\beta 9'\text{Ser} + \text{TQAS-Trp} + 2 \text{ mM FTrp}$   $EC_{50} = 3.4 \pm 0.4$  and  $n_H = 1.3 \pm 0.2$ .  $\alpha 149\text{UAG}\beta 9'\text{Ser} + \text{TQAS-FTrp}$   $EC_{50} = 14 \pm 0.4$  and  $n_H = 1.7 \pm 0.07$ .  $\alpha 149\text{UAG}\beta 9'\text{Ser} + \text{TQAS-FTrp} + 2 \text{ mM FTrp}$   $EC_{50} = 14 \pm 0.7$  and  $n_H = 1.7 \pm 0.1$ . In each experiment  $n > 4$  oocytes. C)  $\alpha 149\text{UAG}$  nonsense suppression and UAARS with FTrp.  $\alpha 149\text{UAG} + \text{TQAS-Trp}$   $EC_{50} = 58 \pm 2$  and  $n_H = 1.7 \pm 0.09$ .  $\alpha 149\text{UAG} + \text{TQAS-Trp} + 2 \text{ mM FTrp}$   $EC_{50} = 76 \pm 7$  and  $n_H = 1.4 \pm 0.06$ .  $\alpha 149\text{UAG} + \text{TQAS-FTrp}$   $EC_{50} = 230 \pm 10$  and  $n_H = 1.4 \pm 0.07$ .  $\alpha 149\text{UAG} + \text{TQAS-FTrp} + 2 \text{ mM FTrp}$   $EC_{50} = 240 \pm 10$  and  $n_H = 1.4 \pm 0.06$ . In each experiment  $n > 3$  oocytes.

To determine whether the placement of FTrp at  $\alpha 149$  was dominating the  $EC_{50}$  shift in UAARS experiments, we chose to combine site-specific incorporation of Trp or FTrp with UAARS with FTrp. Using nonsense suppression at  $\alpha 149\text{UAG}$  results in either 0% FTrp when suppressing with TQAS-W or 100% FTrp when suppressing with TQAS-FTrp. Initially, the  $\beta 9'\text{Ser}$  mutation was utilized to lower the  $EC_{50}$  by a factor of  $\approx 33$ , and the mutation doesn't alter the effect of UAAs incorporated at  $\alpha 149$  (30,31). Suppression of  $\alpha 149\text{UAG}\beta 9'\text{Ser}$  with TQAS-Trp results in an  $EC_{50} = 1.7 \mu\text{M}$  ACh, but suppression of  $\alpha 149\text{UAG}\beta 9'\text{Ser}$  with TQAS-Trp and UAARS with FTrp results in a 2-fold shift in  $EC_{50}$  (Figure 7.6 B). Suppression of  $\alpha 149\text{UAG}\beta 9'\text{Ser}$  with TQAS-FTrp results in an  $EC_{50} = 14 \mu\text{M}$  ACh, but suppression of  $\alpha 149\text{UAG}\beta 9'\text{Ser}$  with TQAS-FTrp

and UAARS with FTrp causes no shift in  $EC_{50}$  (Figure 7.6 B). The  $EC_{50}$  for  $\alpha 149\text{FTrp}\beta 9'\text{Ser}$  is expected to be  $\approx 6 \mu\text{M}$  and it is unclear why the  $EC_{50}$  was higher for these experiments.

We then chose to use the wild-type,  $\beta 9'\text{Leu}$  nAChR, which had been used in previous UAARS experiments. Suppression of  $\alpha 149\text{UAG}$  with TQAS-Trp results in an  $EC_{50} = 58 \mu\text{M}$  ACh, but suppression of  $\alpha 149\text{UAG}$  with TQAS-Trp and UAARS with FTrp results in a 1.3-fold shift in  $EC_{50}$  (Figure 7.6 C). Suppression of  $\alpha 149\text{UAG}$  with TQAS-FTrp results in an  $EC_{50} = 230 \mu\text{M}$  ACh, but suppression of  $\alpha 149\text{UAG}$  with TQAS-FTrp and UAARS with FTrp causes no shift in  $EC_{50}$  (Figure 7.6 C). If  $\alpha 149\text{FTrp}$  was causing the entire shift in  $EC_{50}$ , then both of the suppression experiments (TQAS-Trp or TQAS-FTrp) would be expected to show no shift in  $EC_{50}$  from UAARS.

### 7.2.8 Cross-Linking the nAChR with PLeu and PMet

The UAAs PLeu and PMet are used to detect protein-protein interactions *in vivo* (22). These UAAs are heterogeneously incorporated into all translated proteins and UV irradiation is used to convert the diazirine to a reactive carbene intermediate that irreversibly cross-links either within a protein or to another protein if the UAA is in close proximity. Cross-linked protein complexes are typically detected by Western blotting as an increased molecular weight relative to non-cross-linked protein. We chose to perform Western blots of the  $\alpha_{\text{HA His}}$  (contains the HA tag in the M3-M4 loop and a 6-His tag at the C-terminus) or  $\alpha_{\text{NHA}}$  (contains the HA at the N-terminus). By only detecting the  $\alpha$ -subunit, we would expect to obtain four possible dimers  $\alpha^1\beta$ ,  $\alpha^1\gamma$ ,  $\alpha^2\gamma$  or  $\alpha^2\delta$ ; five possible trimers  $\alpha^1\beta\delta$ ,  $\alpha^1\gamma\alpha^2$ ,  $\gamma\alpha^1\beta$ ,  $\alpha^2\delta\beta$ ,  $\delta\alpha^2\gamma$ ; five possible tetramers  $\alpha^1\gamma\alpha^2\delta$ ,  $\gamma\alpha^1\beta\delta$ ,  $\beta\alpha^1\gamma\alpha^2$ ,  $\alpha^2\beta\delta\alpha^1$ , and  $\beta\delta\alpha^2\gamma$ ; and one pentamer  $\alpha^1\gamma\alpha^2\delta\beta$  (note:  $\alpha^1$  and  $\alpha^2$  are used to show

the uniqueness of the different subunit interfaces of the two  $\alpha$ -subunits). Each subunit of the nAChR runs at a distinct molecular weight (see Figure 6.10), and therefore different subunit combinations may run at different masses. Also, trimers and tetramers with two  $\alpha$ -subunits may be detected more readily because there are two HA tags and should bind two antibodies (Abs).

Oocytes that are supplemented with Leu and Met show no increased molecular weight bands with or without the exposure to UV light (Figure 7.7 A & B, Lanes 2, 3, 6, and 7). Oocytes that were supplemented with PLeu and PMet showed higher molecular weight bands when not irradiated with UV light (Figure 7.7 A & B, Lanes 4 and 8). These higher molecular weight bands are most likely caused by ambient light in the lab. Oocytes that were supplemented with PLeu and PMet and irradiated with UV light for 40 min at room temperature show no high molecular weight bands, but there is a loss of the  $\alpha$ -subunit intensity (Figure 7.7 A & B, Lanes 5 and 9). A similar reduction in  $\alpha$ -subunit intensity is seen for oocytes supplemented with Leu and Met (Figure 7.7 A & B, Lanes 3 and 7). Ponceau staining of the nitrocellulose membrane shows a loss in total protein for oocytes supplemented with PLeu and PMet (Figure 7.7 C & D, Lanes 5 and 9), but there is little loss with oocytes supplemented with Leu and Met (Figure 7.7 C & D, Lanes 3 and 7). Therefore UV irradiation at room temperature may be resulting in  $\alpha$ -subunit and total protein loss by heat with 40 min. Irradiating whole oocytes on the arc lamp (3 min on each sides) shows only faint higher molecular weight bands (Figure 7.7 B, Lane 10) or nothing (Figure 7.7 A, Lane 10), but there appears to be no loss of  $\alpha$ -subunit intensity with fewer UV irradiation periods.

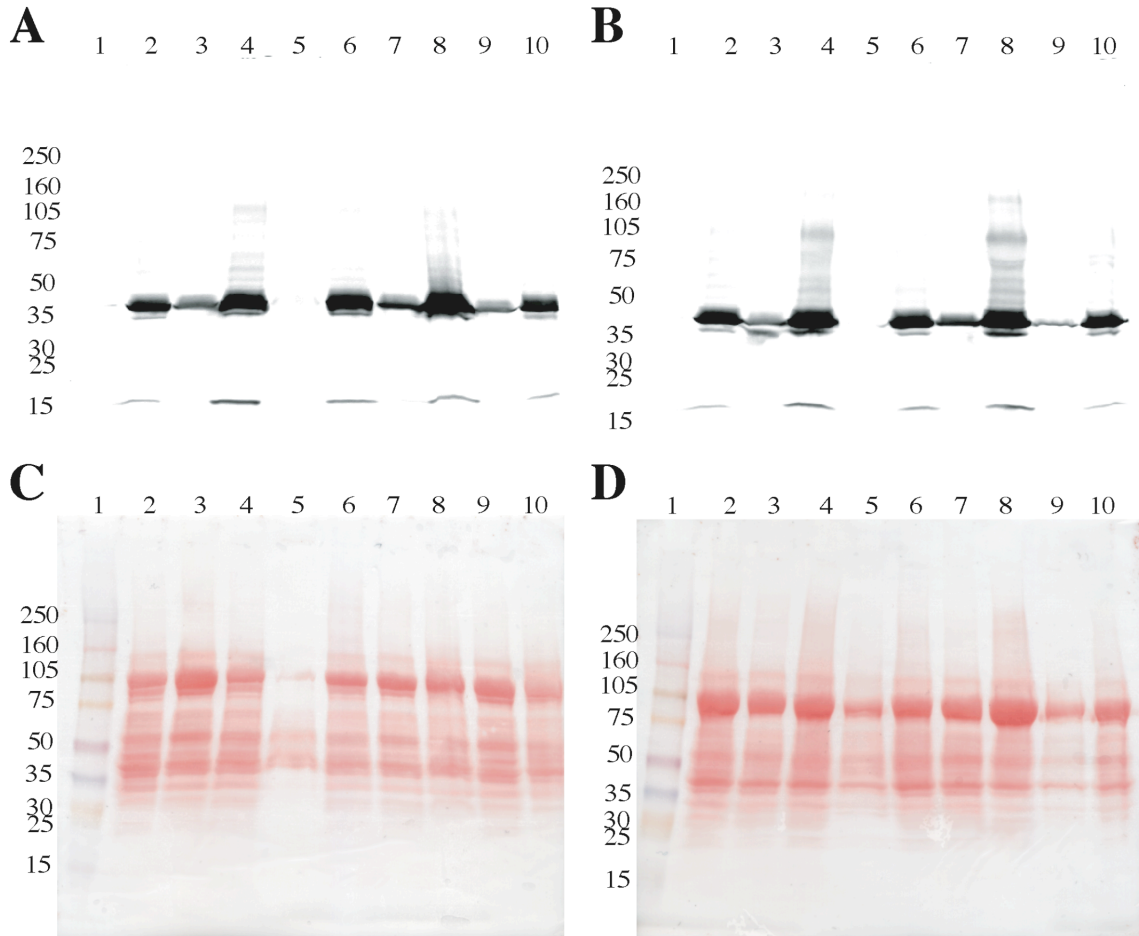


**Figure 7.7:** Detecting cross-linking of  $\alpha_{\text{HA His}}$  with the HA Ab. (A & B) Gels are the same, but with different oocytes. Lane 1 is molecular weight marker. Lane 2 is  $\alpha_{\text{HA His}}$  with 1 mM Leu and 0.5 mM Met. Lane 3 is  $\alpha_{\text{HA His}}$  with 1 mM Leu and 0.5 mM Met irradiated with UV light. Lane 4 is  $\alpha_{\text{HA His}}$  with 1 mM PLeu and 0.5 mM PMet. Lane 5 is  $\alpha_{\text{HA His}}$  with 1 mM PLeu and 0.5 mM PMet irradiated with UV light. Lane 6 is  $\alpha_{\text{HA His}}$  with 1 mM Leu, 0.5 mM Met, and 0.17 mM 18 other aas. Lane 7 is  $\alpha_{\text{HA His}}$  with 1 mM Leu, 0.5 mM Met, and 0.17 mM 18 other aas irradiated with UV light. Lane 8 is  $\alpha_{\text{HA His}}$  with 1 mM PLeu, 0.5 mM PMet, and 0.17 mM 18 other aas. Lane 9 is  $\alpha_{\text{HA His}}$  with 1 mM PLeu, 0.5 mM PMet, and 0.17 mM 18 other aas irradiated with UV light. Lane 10 is  $\alpha_{\text{HA His}}$  with 1 mM PLeu, 0.5 mM PMet, and 0.17 mM 18 other aas irradiated with UV light on the arc lamp (3 min on each side of the oocyte). (C & D) Ponceau staining of Western blots in (A & B). Staining shows loss of total protein after irradiation with UV light. UV irradiation was done 40 min at room temperature (unless otherwise noted). Each lane contains four whole oocytes. Numbers on the left are molecular weight markers (KD).

Cross-linking may hinder detection of the  $\alpha$ -subunit because the HA tag is in the M3-M4 loop and may form secondary structure during cross-linking, such as a loop. The

HA Ab detects a linear sequence of aas and any structure may not allow for detection. We choose to detect the  $\alpha$ -subunit with the His Ab because the 6-His tag is at the C-terminus and is unlikely to cross-link. The  $\alpha_{\text{NHA}}$  was also used because the HA tag is in the N-terminus and is also unlikely to cross-link. Using the same amount of His Ab as the HA antibody, no  $\alpha$ -subunit could be detected (Figure 7.8 A). After stripping the membrane, the membrane was reprobed with the HA, Ab and the  $\alpha$ -subunit is clearly visible (Figure 7.8 B). Oocytes injected with  $\alpha_{\text{HA His}}$  and supplemented with PLeu and PMet show faint higher molecular weight bands without UV irradiation (Figure 7.8 B, Lanes 3 and 9). Intriguingly, no higher molecular weight bands are visualized for oocytes injected with  $\alpha_{\text{HA His}}$  and supplemented with only PLeu (Figure 7.8 B, Lane 5 and 6). The  $\alpha_{\text{NHA}}$  didn't express as well as  $\alpha_{\text{HA His}}$ , and no higher molecular weight bands are seen with or without UV irradiation (Figure 7.8 B, Lanes 7 and 8). Less UV irradiation time (10 min, instead of 40 min as in Figure 7.7) was used to avoid loss of  $\alpha$ -subunit and total protein. Oocytes expressing  $\alpha_{\text{HA His}}$  supplemented with PLeu and PMet only show higher molecular weight bands in Figure 7.8 B, Lane 4. Other oocytes expressing  $\alpha_{\text{HA His}}$  supplemented with PLeu and PMet or only PLeu show no increased molecular weight bands, and there is still a slight reduction in the  $\alpha$ -subunit intensity (Figure 7.8 B, Lanes 6 and 10).

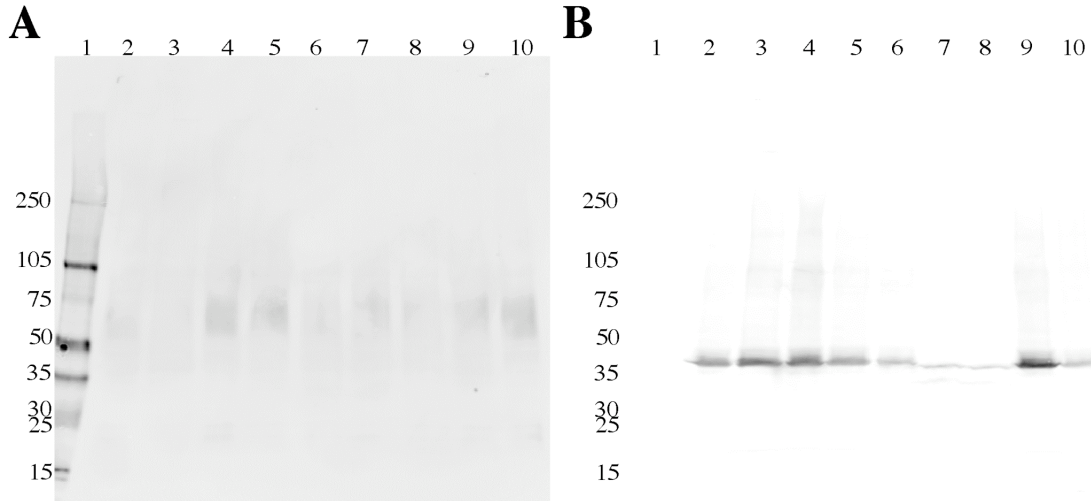


**Figure 7.8:** Detecting cross-linking of  $\alpha_{\text{HA His}}$  with the His Ab and HA Ab. A) Detection of  $\alpha_{\text{HA His}}$  with the His Ab. B) Is the same gel as in A, but detected with the HA Ab after stripping the membrane. (A & B) Lane 1 molecular weight marker. Lane 2 is  $\alpha_{\text{HA His}}$  with 1 mM Leu and 0.5 mM Met. Lane 3 is  $\alpha_{\text{HA His}}$  with 1 mM PLeu and 0.5 mM PMet. Lane 4 is  $\alpha_{\text{HA His}}$  with 1 mM PLeu and 0.5 mM PMet irradiated with UV light. Lane 5 is  $\alpha_{\text{HA His}}$  with 1 mM PLeu. Lane 6 is  $\alpha_{\text{HA His}}$  with 1 mM PLeu irradiated with UV light. Lane 7 is  $\alpha_{\text{NHA}}$  with 1 mM PLeu and 0.5 mM PMet. Lane 8 is  $\alpha_{\text{NHA}}$  with 1 mM PLeu and 0.5 mM PMet irradiated with UV light. Lane 9 is  $\alpha_{\text{HA His}}$  with 1 mM PLeu and 0.5 mM PMet. Lane 10 is  $\alpha_{\text{HA His}}$  with 1 mM PLeu and 0.5 mM PMet irradiated with UV light. UV irradiation was done for 10 min at room temperature. Each lane contains four whole oocytes. Numbers on the left are molecular weight markers (KD).

The loss of  $\alpha$ -subunit intensity with increased molecular weight bands is concerning, and therefore UV irradiation was performed for 2 h at 4 °C. The lack of high molecular weight bands may be due to the minimal amount of nAChR produced in an oocyte (pico-femto grams) and therefore oocytes were homogenized and solubilized for 2 d at 18 °C. Oocytes that were supplemented with Leu and Met show no high molecular weight bands (Figure 7.9 A & B, Lane 2). The large smear running between 75 KD and 105 KD is an abundant protein in the *Xenopus* oocyte (see Figure 7.7 C & D), which is more abundant in this gel because of the 2 d solubilization and is detected because of non-specific HA and/or 2° Ab binding. Oocytes that were supplemented with PLeu and PMet either show higher molecular weight bands (Figure 7.9 A, Lane 3) or no higher

molecular weight bands (Figure 7.9 B, Lane 3) without UV irradiation, the latter is most likely due to minimal protein expression. Oocytes supplemented with PLeu and PMet show higher molecular weight bands with 2 h of UV irradiation (Figure 7.9 A, Lanes 4, 5, 8, and 9, and Figure 7.9 B, Lanes 4–8), but these are not seen in some lanes with lower protein loading (Figure 7.9 A, Lanes 6, 7, and 10, and Figure 7.9 B, 9 and 10). Some lanes also show higher molecular weight bands than a pentamer expected for the nAChR (Figure 7.9 B, Lanes 4–7). Therefore cross-linking of the  $\alpha$ -subunit appears to be minimal in the *Xenopus* oocytes and longer UV irradiation at 4 °C and solubilization is necessary to obtain higher yields of the cross-linked subunits.

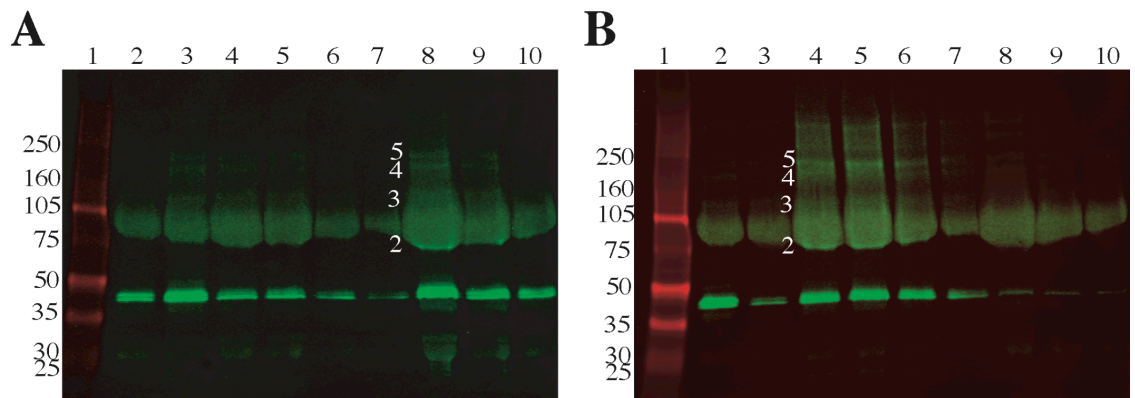


**Figure 7.9:** Detecting cross-linking of  $\alpha_{\text{HA His}}$  with the HA Ab after extended UV irradiation. (A & B) Gels are the same, but with different oocytes. Lane 1 molecular weight marker. Lane 2 is  $\alpha_{\text{HA His}}$  with 1 mM Leu and 0.5 mM Met, half oocyte. Lane 3 is  $\alpha_{\text{HA His}}$  with 1 mM PLeu and 0.5 mM PMet, half oocyte. Lane 4 is  $\alpha_{\text{HA His}}$  with 1 mM PLeu and 0.5 mM PMet irradiated with UV light, one oocyte. Lane 5 is  $\alpha_{\text{HA His}}$  with 1 mM PLeu and 0.5 mM PMet irradiated with UV light, half oocyte. Lane 6 is  $\alpha_{\text{HA His}}$  with 1 mM PLeu and 0.5 mM PMet irradiated with UV light, quarter oocyte. Lane 7 is  $\alpha_{\text{HA His}}$  with 1 mM PLeu and 0.5 mM PMet irradiated with UV light, eighth oocyte. Lane 8 is  $\alpha_{\text{HA His}}$  with 1 mM PLeu and 0.5 mM PMet irradiated with UV light, one oocyte. Lane 9 is  $\alpha_{\text{HA His}}$  with 1 mM PLeu and 0.5 mM PMet irradiated with UV light, half oocyte. Lane 10 is  $\alpha_{\text{HA His}}$  with 1 mM PLeu and 0.5 mM PMet irradiated with UV light, quarter oocyte. UV irradiation was done for 2 h at 4 °C. Numbers on the left are molecular weight markers (KD). Numbers in white are the number of subunits cross-linked.

### 7.2.9 Unnatural Amino Acid Replacement Scanning Expression Determined by Electrophysiology and Western Blot

During the course of the UAARS experiments done in Sections 7.2.2 through 7.2.7, many UAAs showed unusually low current when compared to wild-type nAChR not supplemented with UAAs. To analyze this phenomenon among different batches of oocytes, the average maximal current ( $I_{\max}$ ) from UAARS experiments were normalized to wild-type nAChR  $I_{\max}$ , not supplemented with UAAs. Figure 7.10 shows the variable effect that natural aas and UAAs in the incubation media have on functional expression of ion channels on the membrane of *Xenopus* oocytes. Met, Pro, and Leu are all natural aas and when they are supplemented at 1 mM in the media there is  $\approx 40\%$  reduction in  $I_{\max}$  (Figure 7.10). PMet, Nval, 2Pyr, 3Pyr, 4Pyr, Bth, and Thi all show increased  $I_{\max}$  (Figure 7.10), but PMet, Nval, 4Pyr, Bth, and Thi show no change in  $EC_{50}$  (Table 7.1 and Figure 7.5). Of the Met derivatives, Ppg shows a decrease in  $I_{\max}$ , and PMet and Nval show an increase in  $I_{\max}$  (Figure 7.10). Both Pro derivatives, Aze and Dhp, show a decrease in  $I_{\max}$  equal to the addition of Pro (Figure 7.10). PLeu shows  $I_{\max}$  equivalent to oocytes not supplemented with UAAs, but F3Leu shows a severe reduction in  $I_{\max}$  (Figure 7.10). Intriguingly, *o*FPhe, *m*FPhe, and *p*FPhe all show different  $I_{\max}$  profiles (Figure 7.10). *p*FPhe reduces  $I_{\max}$  by 94%, while *m*FPhe is comparable to Met, Leu, and Pro (Figure 7.10). 3,4-F2Phe shows only a slight reduction in  $EC_{50}$  (Table 7.1), but shows  $I_{\max}$  reduction (57%) that is close to the average reduction of  $I_{\max}$  for *m*FPhe and *p*FPhe (62%) (Figure 7.10). 3,5-F2Phe, F3Phe, and F5Phe showed no change in  $EC_{50}$  (Table 7.1) and the reduction in  $I_{\max}$  is similar to Met, Leu, and Pro (Figure 7.10). FVal and

FTrp also cause a reduction in  $I_{\max}$  (Figure 7.10). Overall, fluorinated UAAs appear to reduce the functional nAChR on the surface of the oocyte membrane (Figure 7.10).

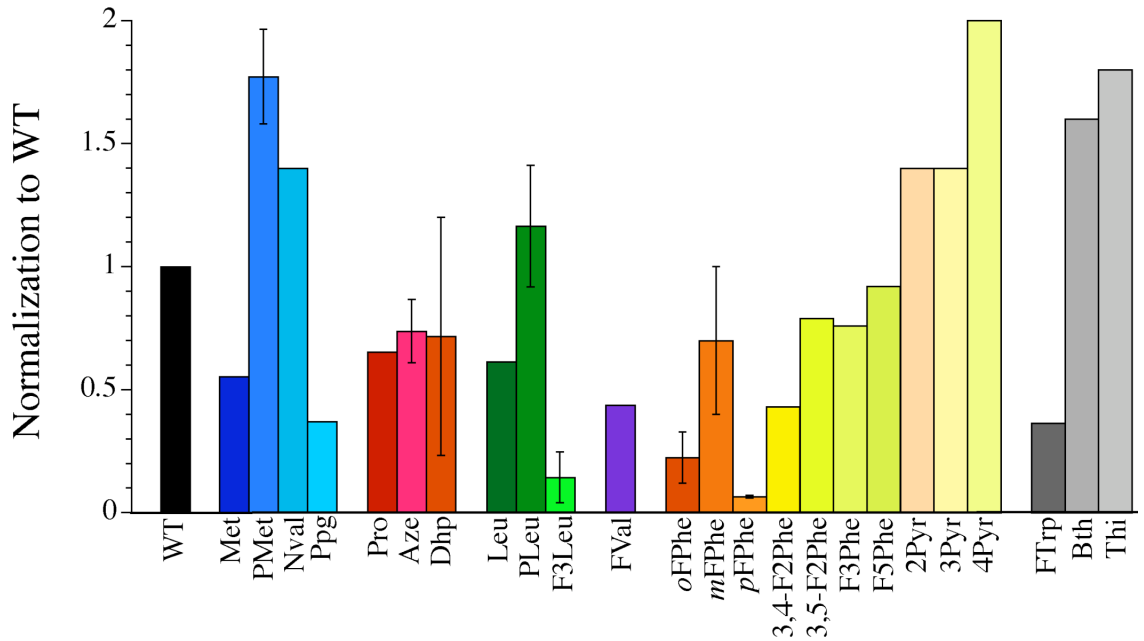


**Figure 7.10:** UAARS effect on functional nAChR expression detected by electrophysiology.  $I_{\max}$  for UAARS experiments was normalized to  $I_{\max}$  for nAChR without UAAs. WT is wild-type nAChR and natural aas or UAAs (chemical structure shown in Figure 7.1) are listed below each bar. Error bars are standard error.

To determine whether UAARS causes decreased nAChR translation or increased protein degradation, whole cell homogenization and Western blot were utilized to look at  $\alpha$ -subunit protein. Figure 7.11 A shows that the  $\alpha$ -subunit is translated and present in oocytes equally without UAAs in the media (Figure 7.11 A, Lane 2) and in the presence of UAAs (Figure 7.11 A, Lanes 3–10). Densitometric analysis of Figure 7.11 A confirms that *o*FPhe, *m*FPhe, *p*FPhe, FTrp, and FVal all have the same amount of  $\alpha$ -subunit as oocytes not supplemented with UAAs (Figure 7.11 B). Therefore reduction of  $I_{\max}$  for these UAAs (Figure 7.10) is not due to decreased translation or protein degradation, but rather another mechanism.

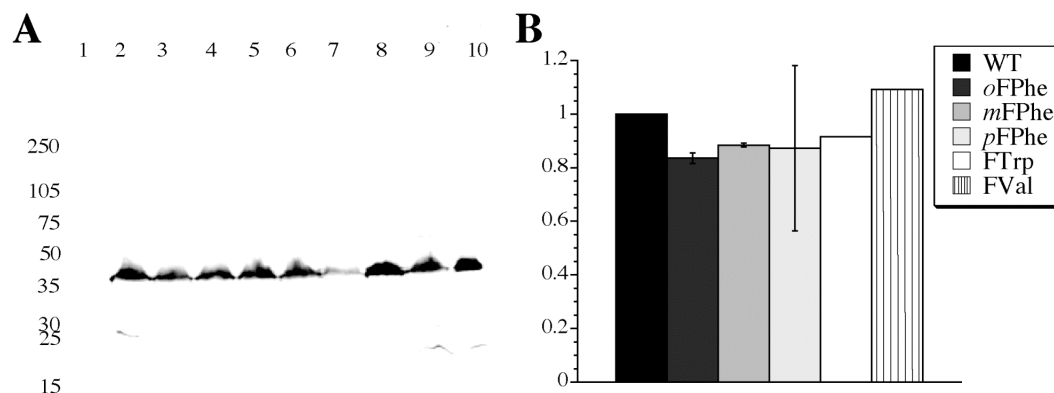


**Figure 7.11:** UAARS effect on nAChR expression detected by Western blot. A) UAARS with *o*FPhe, *m*FPhe, *p*FPhe, FTrp, and FVal. Lane 1 molecular weight marker. Lane 2 is  $\alpha_{\text{HA His}}$ . Lanes 3 and 4 are  $\alpha_{\text{HA His}}$  with 1 mM *o*FPhe. Lanes 5 and 6 are  $\alpha_{\text{HA His}}$  with 1 mM *m*FPhe. Lanes 7 and 8 are  $\alpha_{\text{NHA}}$  with 1 mM *p*FPhe. Lane 9 is  $\alpha_{\text{HA His}}$  with 2 mM FTrp. Lane 10 is  $\alpha_{\text{HA His}}$  with 2 mM FVal. Each lane contains four whole oocytes. Numbers on the left are molecular weight markers (KD). B) Densitometric analysis of Western blot in part A. Signal intensity was normalized to  $\alpha_{\text{HA His}}$  not supplemented with UAAs (Lane 2). Error bars are standard error.

### 7.3 Discussion

UAARS requires depletion of the endogenous aas for efficient incorporation of UAAs (shown schematically in Figure 7.2). This is experimentally shown by the increased shift in  $EC_{50}$  for PLeu and F3Leu from 2 to 5 d incubations (Figure 7.4 B). Injection of PLeu and PMet (final concentration in an oocyte 1 mM and 0.5 mM, respectively) caused no shift in  $EC_{50}$  of the nAChR and resulted in  $\approx 50\%$  reduction in nAChR expression when determined by electrophysiology (data not shown). Therefore the use of excess UAAs in the media is needed for increased UAA concentration in the oocyte and for efficient UAARS.

Many UAAs showed no shift in  $EC_{50}$ , which may be due to lack of efficient UAA incorporation by the translational machinery, lack of UAA recognition by aaRSs, or no change in nAChR function. Increased incubation times are required to get significant

shifts for Aze, which may be required for 3,4-F2Phe (Table 7.1). F5Phe was not recognized in *E. coli* (15) and therefore may also not be in *Xenopus* oocytes. The Met derivatives (PMet, Nval, and Ppg) all showed no shift in EC<sub>50</sub> (Table 7.1) and other ion channels (5HT<sub>3A</sub>, GABA<sub>A</sub>, MOD-1, etc.) may be useful to screen for these Met derivatives. With increased research on other ion channels, hopefully UAARS EC<sub>50</sub> shifts can be determined for all 20 canonical aas (or 19 if Gly is omitted) to allow efficient screening of all UAA derivatives. Other methods of detection will also be useful, including bioorthogonal labeling of UAAs with fluorophores (23,24,42) and detection by total internal reflectance microscopy (TIRF) (43). TIRF will not only show the presence of UAAs, but can also be used to count the number of accessible UAAs of a single nAChR and can be used to determine the distribution of UAAs incorporated into nAChRs.

The commercially available PLeu causes a change in the function of the nAChR, but no shift is seen with PMet (Figure 7.4 A). PLeu is hydrophilic compared to F3Leu, but both UAAs cause a GOF phenotype in the nAChR (Figure 7.4 B). This is intriguing, because Leu is the most abundant UAA in the nAChR and Leu is a hydrophobic aa thought to stabilize the interior of proteins and to interact with the lipid bilayer (Figure 7.3). The two UAAs—PLeu and F3Leu—are distinguishable by the number of functional ion channels present on the surface. The hydrophilic PLeu results in comparable expression to wild-type nAChR not supplemented with UAAs, but the hydrophobic F3Leu results in a 86% reduction in current (Figure 7.10). This may result from differential interactions with chaperones, interactions with lipid bilayers in the endoplasmic reticulum and/or golgi, folding by the translocon, change in conductance, or

differences in the amount of functional receptors for each UAA. Val is another hydrophobic aa and is present comparably to Leu in the nAChR (Figure 7.3). The incorporation of the more hydrophobic FVal results in a LOF phenotype (Table 7.1), which contrasts to the GOF phenotype of PLeu and F3Leu. Expression of functional ion channels is decreased by 56% with FVal and is similar to F3Leu (Figure 7.10). Further research on hydrophobic residues will be intriguing on the nAChR because they are so abundant, contact subunit interfaces, and interact with the lipid bilayer (Figure 7.3).

Phe is the most abundant aromatic aa in the nAChR and forms extensive interactions with the lipid bilayer (Figure 7.3). Fluorination of Phe decreases the cation- $\pi$  binding ability of the phenyl ring (44), but also places a highly electronegative substituent and increases the hydrophobicity of the side chain. Intriguingly, fluorination of the *ortho*, *meta*, and *para* positions of Phe have different effects on the function of the nAChR. *o*FPhe causes a LOF phenotype, *m*FPhe causes a slight GOF phenotype, and *p*FPhe causes the greatest GOF phenotype of UAAs screened (Figure 7.5 A). The pyridylalanine derivatives have decreased cation- $\pi$  binding ability as well (44), but also remove a H atom and increase hydrophilicity of the side chain. 2Pyr results in a LOF phenotype similar to *o*FPhe (Figure 7.5 A & B). 3Pyr results in a GOF phenotype similar to *m*FPhe (Figure 7.5 A & B). 4Pyr shows no shift in  $EC_{50}$  (Figure 7.5 B), which is either due to possible protonation of 4Pyr or evidence that the loss of a H atom doesn't influence the function of the nAChR. Fluorination of the *para* position on *p*FPhe causes a significant shift in  $EC_{50}$ , which greatly alters nAChR function. These UAAs show distinct interactions of the Phe side chain and clearly illustrate that the *ortho*, *meta*, and *para* positions have differential interactions within the nAChR and/or the lipid bilayer.

Trp is the least used aromatic aa in the nAChR (Figure 7.3), and in proteins in general. UAARS with FTrp results in a LOF phenotype similar to the site-specific incorporation of FTrp at  $\alpha$ 149 (Figure 7.6 A). 4-FTrp and 6-FTrp are accepted by *E. coli* (19) and these derivatives should be intriguing to see if there is a functional difference on the nAChR similar to the Phe derivatives. Differences in  $EC_{50}$  shift have been seen at  $\alpha$ 149 in the nAChR, where site-specific incorporation of 4-FTrp and 6-FTrp cause no shift in  $EC_{50}$ , but 5-FTrp (FTrp) cause a 4-fold shift in  $EC_{50}$  (30). Combining site-specific UAA incorporation with UAARS allows for a novel experimental technique to remove one position from UAARS. Using  $\alpha$ 149UAG and suppressing with TQAS-W, 0% of the ion channels will contain FTrp at this position and there is still a LOF phenotype seen with UAARS with FTrp (Figure 7.6 B & C), although significantly smaller than that from simple UAARS. Intriguingly, suppressing  $\alpha$ 149UAG with TQAS-FTrp (100% of the ion channels will have FTrp at  $\alpha$ 149) shows no shift in  $EC_{50}$  (Figure 7.6 B & C). Both experiments should show a shift in  $EC_{50}$  if there is a global change in function with UAARS with FTrp or no shift if the  $\alpha$ 149FTrp position is dominating the shift in  $EC_{50}$ . This difference may be explained by a positional affect near the ACh binding site, known as the aromatic box.  $\alpha$ 149Trp may show a shift because FTrp at the only other Trp in the aromatic box may alter ACh binding, but  $\alpha$ 149FTrp may dominate the reduction in ACh binding and FTrp at the other site has no effect. Further research is needed to explain this phenomenon, but clearly illustrates the utility of combining site-specific UAA incorporation with UAARS.

PLeu and PMet allow for detection of UAA incorporation by cross-linking subunits within the nAChR upon UV irradiation and detection of higher molecular weight

bands on a Western blot. Detection of  $\alpha_{\text{HA His}}$  was not possible with the His Ab (Figure 7.8 A) and clearly illustrates the difficulty in detecting a low abundance ion channel with Abs other than the HA Ab from Covance. Wild-type nAChR supplemented with Leu and Met show no higher molecular weight bands with and without UV irradiation (Figure 7.7 A & B, Lanes 2, 3, 6, and 7, Figure 7.8 B, Lane 2, and Figure 7.9 A & B, Lane 2). nAChR supplemented with PLeu and PMet show higher molecular weight bands without UV irradiation, even though the oocytes are kept in an opaque box and only exposed to light during media exchange and homogenization (Figure 7.7 A & B, Lanes 4 and 8, Figure 7.8 B, Lanes 3 and 9, and Figure 7.9 A, Lane 3). This suggests that many Leu and/or Met positions of the nAChR are in close contact with other subunits. nAChR supplemented with PLeu and PMet sometimes show higher molecular weight bands with UV irradiation (Figure 7.8 B, Lane 4, Figure 7.9 A, Lanes 4, 5, 8, and 9, and Figure 7.9 B, Lanes 4–8). The detection of higher molecular weight bands is highly variable, but is seen more readily with UV irradiation for 2 h at 4 °C and solubilization of whole oocytes for 2 d at 18 °C (Figure 7.9 A, Lanes 4, 5, 8, and 9, and Figure 7.9 B, Lanes 4–8). When the nAChR is supplemented with PLeu only, no higher molecular weight bands are seen with or without UV irradiation (Figure 7.9 B, Lanes 5 and 6). This suggests that PMet is critical for cross-linking of the nAChR. The nAChR is a pentamer, but occasionally higher molecular weight bands were seen (Figure 7.9 B, Lanes 4–7). Cross-linking of the nAChR requires highly specialized conditions in order to maximize the yield of the cross-linked subunits, which are present in extremely low yield and/or difficult to solubilize. UAARS with PLeu and PMet can be detected by Western blot, but cross-linking is inefficient and highly variable.

The supplementation of natural aas and UAAs (0.5–4 mM) effects the functional expression of the nAChR. 1 mM of Leu, Met, and Pro all decrease expression by  $\approx 40\%$  relative to oocytes not supplemented with natural aas (Figure 7.10). The decrease in channel expression may be caused by overwhelming the translation machinery through increased concentration of natural aas, which increases aminoacylated tRNAs, imbalances the aminoacylated tRNA pool and portion bound to EF-1 $\alpha$ , and could cause ribosomal stalling, increased frameshifting, and protein truncation. P<sub>Met</sub> and N<sub>val</sub> both *increase* expression by 77% and 40%, respectively (Figure 7.10). This suggests that the Met concentration in *Xenopus* oocytes is not optimal for nAChR expression and the increase of P<sub>Met</sub> and N<sub>val</sub> may also increase translation and/or initiation of translation. This may be useful for increasing nAChR translation and/or site-specific UAA incorporation experiments by supplementation of Met (< 1 mM) or Met derivatives. D<sub>hp</sub> and A<sub>ze</sub> result in  $\approx 40\%$  decrease in functional channel expression, which is similar to Pro (Figure 7.10). *o*F<sub>Phe</sub> and *p*F<sub>Phe</sub> show 88% and 93%, respectively, reduction in expression, while *m*F<sub>Phe</sub> shows 30% reduction (Figure 7.10). 3,5-F<sub>2</sub>P<sub>he</sub>, F<sub>3</sub>P<sub>he</sub>, and F<sub>5</sub>P<sub>he</sub> (no shift in EC<sub>50</sub> Table 7.1) all show  $\approx 20\%$  reduction in functional channel expression, while 3,4-F<sub>2</sub>P<sub>he</sub> shows a 57% reduction and suggests incorporation (Figure 7.10). 2P<sub>yr</sub> and 3P<sub>yr</sub> show 50% increase in expression, while 4P<sub>yr</sub> shows a 100% increase in expression (Figure 7.10). B<sub>th</sub> and T<sub>hi</sub> show an 60% and 80% increase in expression (Figure 7.10) even though there is no shift in EC<sub>50</sub> (Table 7.1). Of the UAAs that caused a shift in EC<sub>50</sub>, UAARS with fluorinated UAAs (F<sub>3</sub>Leu, F<sub>Val</sub>, F<sub>Trp</sub>, *o*F<sub>Phe</sub>, *m*F<sub>Phe</sub>, and *p*F<sub>Phe</sub>) appears to decrease functional ion channel expression relative to non-fluorinated UAAs (P<sub>Leu</sub>, 2P<sub>yr</sub>, and 3P<sub>yr</sub>) (Figure 7.10). Intriguingly, there is no change

in the total  $\alpha$ -subunit when detected by Western blot for *o*FPhe, *m*FPhe, *p*FPhe, FTrp, and FVal (Figure 7.11). Therefore the UAA incorporation doesn't cause decreased translation or increased protein degradation, but most likely the channels are not functional, have altered conductance, or are not present on the cell surface (remain sequestered in the endoplasmic reticulum, golgi, or vesicles). Western blots of the membrane only can further elucidate where the nAChR is located. Natural aas and UAAs supplemented in the media effect functional nAChR expression, but appear not to diminish protein translation for tested fluorinated UAAs.

UAARS is a useful method for analyzing the global effect of UAA incorporation. The commercially available UAA PLeu alters nAChR function and caution should be observed when heterogeneously incorporating UAAs. Further research is necessary to extend UAARS to other ion channels to try and attain shifts for the 20 natural aas (or 19 if Gly is omitted). UAARS with UAAs not used in this research will further extend trends discussed and gain further insight into aa function in the nAChR. Extension of UAARS to charged and polar aas will also be interesting to see the effect on the function of the nAChR. UAARS is a useful technique for evaluating whether the translational machinery of the *Xenopus* oocyte accepts an UAA. UAAs that are accepted by the translational machinery require site-specific incorporation by chemically aminoacylated tRNAs, but UAAs that are not accepted can be incorporated by evolved aminoacyl synthetase/tRNA pairs for site-specific UAA incorporation. The use of *E. coli* mutant aaRS can be useful to incorporate UAAs that are not recognized by the endogenous aaRS (site-specific or statistical incorporation) and can also be utilized with a specific isoacceptor *E. coli* tRNA to only incorporate UAAs at a subset of triplet codons.

UAARS with multiple UAAs will lead to diverse populations of nAChR and can be used to look at specific interactions between classes of aas, such as salt bridges (Lys/Arg and Glu/Asp). UAARS combined with site-specific UAA incorporation should be a useful technique for analyzing whether specific sites dominate functional changes. The UAARS method is an intriguing technique that should have many applications in *Xenopus* oocytes for many different proteins.

## 7.4 Experimental Methods

### 7.4.1 Materials

T7 mMessage mMachine kits were from Ambion (Austin, TX). ACh chloride and yeast inorganic pyrophosphatase were purchased from Sigma-Aldrich. HA.11 monoclonal antibody from mouse was from Covance (Berkeley, CA). IRDye<sup>TM</sup>800CW conjugated affinity purified anti-mouse IgG from goat was from Rockland (Gilbertsville, PA). Mouse anti-His antibody was from Amersham Biosciences (Piscataway, NJ). 5-Fluoro-DL-Tryptophan (FTrp) was from Acros (Geel, Belgium). 5,5,5-Trifluoro-DL-leucine (F3Leu) was from Alfa Aesar (Ward Hill, MA). H-3,4-Dehydro-L-Proline (Dhp) and L-Azetidine-2-Carboxylic Acid (Aze) were from Chem-Impex Int (Wood Dale, IL). 3-Fluoro-DL-Valine (FVal) was from Fluka (Seelze, Germany). L-2-Fluorophe (*o*FPhe), L-3-Fluorophe (*m*FPhe), L-4-Fluorophe (*p*FPhe), L-3,4-Difluorophe (3,4-F2Phe), L-3,5-Difluorophe (3,5-F2Phe), L-2,4,5-Trifluorophe (F3Phe), L-Pentafluorophe (F5Phe), L-2-Pyridylalanine (2Pyr), L-3-Pyridylalanine (3Pyr), L-4-Pyridylalanine (4Pyr), L-Propargylglycine (Ppg), (R)-2-Thienylglycine (Thi), and L-3-Benzothienylalanine (Bth)

were from Peptech (Burlington, MA). L-Photo-Leucine (PLeu), L-Photo-Methionine (PMet), and dialyzed FBS were from Pierce (Rockford, IL).

#### **7.4.2 nAChR Gene Preparation and mRNA Transcription**

The masked  $\alpha_{\text{NHA}}$ -,  $\beta$ -,  $\gamma$ -, and  $\delta$ -subunits (all ending with the ochre (UAA) stop codon) of the nAChR subcloned in the pAMV vector were previously prepared (45,46). The  $\alpha_{\text{HA His}}$  in the pAMV vector was previously prepared (36). DNA was linearized with NotI (New England Biolabs) and mRNA was prepared with the T7 mMessage mMachine kit with 0.5  $\mu\text{l}$  of yeast inorganic pyrophosphatase. mRNA was purified using the RNeasy Mini kit (Qiagen, Valencia, CA) and quantified by absorption at 260 nm.

#### **7.4.3 *In Vivo* nAChR Expression, UAARS, and Site-Specific UAA Incorporation**

Stage VI oocytes of *Xenopus laevis* were prepared as described (47). Oocytes were incubated at 18 °C for 41–56 h (unless otherwise stated in the figure legends). 2 ng of mRNA in a subunit ratio of 2:1:1:1 for  $\alpha_{\text{HA His}}$  or  $\alpha_{\text{NHA}}:\beta:\gamma:\delta$  was injected for 2 d incubations, and 1 ng of mRNA in the same subunit ratio was injected for 5 d incubations. UAAs were added to ND96 with  $\text{Ca}^{2+}$  and 5% FBS immediately prior to injection. After injection, oocytes were divided equally among all dishes containing exactly 4 mL of solution. Media was changed every 24 h after injection. For  $\alpha$ 149UAG ( $\beta$ 9'Ser) nonsense suppression, 40 ng of mRNA in a subunit ratio of 10:1:1:1  $\alpha$ 149UAG: $\beta$ (or  $\beta$ 9'Ser): $\gamma$ : $\delta$  was injected with 7.5 ng of deprotected TQAS-Trp or TQAS-FTrp (as described in Chapter 5 and (46)). Prior to nonsense suppression the oocytes were incubated in 2 mM FTrp for 24 h and after injection oocytes were incubated for 2 d. For PLeu and PMet experiments, oocytes were kept in an opaque box and exposed to ambient light only during media exchange and homogenization.

#### 7.4.4 Electrophysiology

Recordings employed two-electrode voltage clamp on the OpusXpress 6000A (Molecular Devices). ACh was stored at -20 °C as a 1 M stock, diluted in Ca<sup>2+</sup>-free ND96, and delivered to oocytes by computer-controlled perfusion system. For all experiments, the holding potential was -60 mV. Dose-response data were obtained from at least 12 ACh concentrations. Dose-response relations were fit to the Hill equation to determine EC<sub>50</sub> and the Hill coefficient ( $\eta_H$ ). All reported values are represented as a mean  $\pm$  SE of the tested oocytes (number (n) listed with each table).

#### 7.4.5 UV Irradiation

Oocytes were placed in a dish containing ND96 (no FBS or UAAs) and placed on an orbital shaker. Oocytes were UV irradiated with a 100 W Blak-Ray Lamp (UVP Inc.) with conditions listed with each figure. For arc lamp UV irradiation, oocytes were placed in a 1.5 ml eppendorf and were irradiated through the open end of the eppendorf.

#### 7.4.6 Whole Oocyte Homogenization

Whole oocyte homogenization was performed by placing four oocytes (either immediately from 18 °C incubator or after storage at -80 °C) in a 1.5 ml eppendorf and removing excess ND96. 10  $\mu$ l of homogenization buffer (100 mM NaCl, 50 mM Tris pH = 7.9, 0.6% SDS (w/v), 35 mM *n*-dodecyl  $\beta$ -D-maltoside (DDM) (Anatrace), and 1 protease inhibitor tablet (Roche)) were added to the oocytes, and oocytes were lysed manually with a pipette tip. The solution was sonicated for 10 min and centrifuged for 30 min to remove insoluble debris. The supernatant was transferred to a new eppendorf and 10  $\mu$ l of 2X loading buffer was added. Samples were either stored at -80 °C or run on a gel. For PLeu and PMet 2 d solubilization, the oocytes were homogenized manually

as described above, placed in an eppendorf rack covered in aluminum foil, and placed in 18 °C incubator for 2 d.

#### 7.4.6 Western Blotting of Proteins Expressed in *Xenopus* Oocytes

Western blotting was performed as previously described (37). Briefly 20 µl of samples were loaded on a 4–15% linear gradient, polyacrylamide ready gel Tris-HCl (Bio-Rad) and run at 150 V for 1.25 h. Protein was transferred to nitrocellulose (Bio-Rad) at 30 V for 30 min and 100 V for 1.5 h. Nitrocellulose was blocked overnight using non-fat dairy milk (NFDM) in 1X PBS / 0.1% Tween. 12.5 µl of 1° Ab anti-HA from mouse (or 14.9 µl, for same µg as HA Ab, of 1° Ab anti-His from mouse) was placed in 15 ml NFDM / 1X PBS / 0.1% Tween for 1h, washed 4X with 30 ml 1X PBS / 0.1% Tween for 5 min each, placed in 3 µl 2° 800CW goat anti-mouse IgG in 15 mL NFDM / 1X PBS / 0.1% Tween for 1 h, and washed 4X with 30 ml 1X PBS / 0.1% Tween for 5 min each. Nitrocellulose was visualized using two-color infrared dye detection on the Odyssey (Li-Cor, Lincoln, NE) (Hsieh-Wilson lab). Densitometric analysis was performed using the Li-Cor Odyssey software package.

## 7.5 References

1. Montclare, J.K., and Tirrell, D.A. (2006) Evolving proteins of novel composition. *Angew. Chem. Int. Ed. Engl.*, **45**, 4518–4521.
2. Link, A.J., and Tirrell, D.A. (2005) Reassignment of sense codons *in vivo*. *Methods*, **36**, 291–298.
3. Link, A.J., Mock, M.L., and Tirrell, D.A. (2003) Non-canonical amino acids in protein engineering. *Curr. Opin. Biotechnol.*, **14**, 603–609.

4. Beene, D.L., Dougherty, D.A., and Lester, H.A. (2003) Unnatural amino acid mutagenesis in mapping ion channel function. *Curr. Opin. Neurobiol.*, **13**, 264–270.
5. Dougherty, D.A. (2000) Unnatural amino acids as probes of protein structure and function. *Curr. Opin. Biotechnol.*, **4**, 645–652.
6. Budisa, N. (2004) Prolegomena to future experimental efforts on genetic code engineering by expanding its amino acid repertoire. *Angew. Chem. Int. Ed. Engl.*, **43**, 6426–6463.
7. Wang, L., Xie, J., and Schultz, P.G. (2006) Expanding the genetic code. *Annu. Rev. Biophys. Biomol. Struct.*, **35**, 225–249.
8. Yoshikawa, E., Fournier, M.J., Mason, T.L., and Tirrell, D.A. (1994) Genetically engineered fluoropolymers. Synthesis of repetitive polypeptides containing *p*-fluorophenylalanine residues. *Macromolecules*, **27**, 5471–5475.
9. Deming, T.J., Fournier, M.J., Mason, T.L., and Tirrell, D.A. (1996) Structural modification of a periodic polypeptide through biosynthetic replacement of proline with azetidine-2-carboxylic acid. *Macromolecules*, **29**, 1442–1444.
10. Deming, T.J., Fournier, M.J., Mason, T.L., and Tirrell, D.A. (1997) Biosynthetic incorporation and chemical modification of alkene functionality in genetically engineered polymers. *J. Macromol. Sci. Pure Appl. Chem.*, **34**, 2143–2150.
11. van Hest, J.C., and Tirrell, D.A. (1998) Efficient introduction of alkene functionality into proteins *in vivo*. *FEBS Lett.*, **428**, 68–70.

12. van Hest, J.C.M., Kiick, K.L., and Tirrell, D.A. (2000) Efficient incorporation of unsaturated methionine analogues into proteins *in vivo*. *J. Am. Chem. Soc.*, **122**, 1282–1288.
13. Kiick, K.L., Weberskirch, R., and Tirrell, D.A. (2001) Identification of an expanded set of translationally active methionine analogues in *Escherichia coli*. *FEBS Lett.*, **502**, 25–30.
14. Niemz, A., and Tirrell, D.A. (2001) Self-association and membrane-binding behavior of melittins containing trifluoroleucine. *J. Am. Chem. Soc.*, **123**, 7407–7413.
15. Kirshenbaum, K., Carrico, I.S., and Tirrell, D.A. (2002) Biosynthesis of proteins incorporating a versatile set of phenylalanine analogues. *Chembiochem.*, **3**, 235–377.
16. Minks, C., Huber, R., Moroder, L., and Budisa, N. (2000) Noninvasive tracing of recombinant proteins with "fluorophenylalanine-fingers". *Anal. Biochem.*, **284**, 29–34.
17. Tang, Y., Ghirlanda, G., Petka, W.A., Nakajima, T., DeGrado, W.F., and Tirrell, D.A. (2001) Fluorinated coiled-coil proteins prepared *in vivo* display enhanced thermal and chemical stability. *Angew. Chem. Int. Ed. Engl.*, **40**, 1494–1496.
18. Koide, H., Yokoyama, S., Katayama, Y., Muto, Y., Kigawa, T., Kohno, T., Takusari, H., Oishi, M., Takahashi, S., Tsukumo, K. *et al.* (1994) Receptor-binding affinities of human epidermal growth factor variants having unnatural amino acid residues in position 23. *Biochemistry*, **33**, 7470–7476.

19. Pratt, E.A., and Ho, C. (1975) Incorporation of fluorotryptophans into proteins of *Escherichia coli*. *Biochemistry*, **14**, 3035–3040.
20. Hartman, M.C., Josephson, K., and Szostak, J.W. (2006) Enzymatic aminoacylation of tRNA with unnatural amino acids. *Proc. Natl. Acad. Sci. USA*, **103**, 4356–4361.
21. Hartman, M.C., Josephson, K., Lin, C.W., and Szostak, J.W. (2007) An expanded set of amino acid analogs for the ribosomal translation of unnatural peptides. *PLoS ONE*, **2**, e972.
22. Suchanek, M., Radzikowska, A., and Thiele, C. (2005) Photo-leucine and photo-methionine allow identification of protein-protein interactions in living cells. *Nat. Methods*, **2**, 261–267.
23. Dieterich, D.C., Link, A.J., Graumann, J., Tirrell, D.A., and Schuman, E.M. (2006) Selective identification of newly synthesized proteins in mammalian cells using bioorthogonal noncanonical amino acid tagging (BONCAT). *Proc. Natl. Acad. Sci. USA*, **103**, 9482–9487.
24. Beatty, K.E., Liu, J.C., Xie, F., Dieterich, D.C., Schuman, E.M., Wang, Q., and Tirrell, D.A. (2006) Fluorescence visualization of newly synthesized proteins in mammalian cells. *Angew. Chem. Int. Ed. Engl.*, **45**, 7364–7367.
25. Son, S., Tanrikulu, I.C., and Tirrell, D.A. (2006) Stabilization of bzip peptides through incorporation of fluorinated aliphatic residues. *ChemBiochem.*, **7**, 1251–1257.

26. Tang, Y., Ghirlanda, G., Vaidehi, N., Kua, J., Mainz, D.T., Goddard, I.W., DeGrado, W.F., and Tirrell, D.A. (2001) Stabilization of coiled-coil peptide domains by introduction of trifluoroleucine. *Biochemistry*, **40**, 2790–2796.
27. Tang, Y., and Tirrell, D.A. (2001) Biosynthesis of a highly stable coiled-coil protein containing hexafluoroleucine in an engineered bacterial host. *J. Am. Chem. Soc.*, **123**, 11089–11090.
28. Cirino, P.C., Tang, Y., Takahashi, K., Tirrell, D.A., and Arnold, F.H. (2003) Global incorporation of norleucine in place of methionine in cytochrome P450 BM-3 heme domain increases peroxygenase activity. *Biotechnol. Bioeng.*, **83**, 729–734.
29. Lummis, S.C., Beene, D.L., Lee, L.W., Lester, H.A., Broadhurst, R.W., and Dougherty, D.A. (2005) *Cis-trans* isomerization at a proline opens the pore of a neurotransmitter-gated ion channel. *Nature*, **438**, 248–252.
30. Zhong, W., Gallivan, J.P., Zhang, Y., Li, L., Lester, H.A., and Dougherty, D.A. (1998) From ab initio quantum mechanics to molecular neurobiology: A cation- $\pi$  binding site in the nicotinic receptor. *Proc. Natl. Acad. Sci. USA*, **95**, 12088–12093.
31. Kearney, P.C., Zhang, H., Zhong, W., Dougherty, D.A., and Lester, H.A. (1996) Determinants of nicotinic receptor gating in natural and unnatural side chain structures at the M2 9' position. *Neuron*, **17**, 1221–1229.
32. Chung, H.H., Benson, D.R., Cornish, V.W., and Schultz, P.G. (1993) Probing the role of loop 2 in Ras function with unnatural amino acids. *Proc. Natl. Acad. Sci. USA*, **90**, 10145–10149.

33. Cornish, V.W., Kaplan, M.I., Veenstra, D.L., Kollman, P.A., and Schultz, P.G. (1994) Stabilizing and destabilizing effects of placing beta-branched amino acids in protein alpha-helices. *Biochemistry*, **33**, 12022–12031.
34. Koh, J.T., Cornish, V.W., and Schultz, P.G. (1997) An experimental approach to evaluating the role of backbone interactions in proteins using unnatural amino acid mutagenesis. *Biochemistry*, **36**, 11314–11322.
35. Steiner, T., Hess, P., Bae, J.H., Wiltschi, B., Moroder, L., and Budisa, N. (2008) Synthetic biology of proteins: Tuning GFPs folding and stability with fluoroproline. *PLoS ONE*, **3**, e1680.
36. Leite, J.F., Blanton, M.P., Shahgholi, M., Dougherty, D.A., and Lester, H.A. (2003) Conformation-dependent hydrophobic photolabeling of the nicotinic receptor: Electrophysiology-coordinated photochemistry and mass spectrometry. *Proc. Natl. Acad. Sci. USA*, **100**, 13054–13059.
37. England, P.M., Zhang, Y.N., Dougherty, D.A., and Lester, H.A. (1999) Backbone mutations in transmembrane domains of a ligand-gated ion channel: Implications for the mechanism of gating. *Cell*, **96**, 89–98.
38. Dumont, J.N. (1972) Oogenesis in *Xenopus laevis* (Daudin). I. Stages of oocyte development in laboratory maintained animals. *J. Morphol.*, **136**, 153–179.
39. Weber, W. (1999) Ion currents of *Xenopus laevis* oocytes: State of the art. *Biochim. Biophys. Acta.*, **1421**, 213–233.
40. Taylor, P.M., Kaur, S., Mackenzie, B., and Peter, G.J. (1996) Amino-acid-dependent modulation of amino acid transport in *Xenopus laevis* oocytes. *J. Exp. Biol.*, **199**, 923–931.

41. Miyazawa, A., Fujiyoshi, Y., and Unwin, N. (2003) Structure and gating mechanism of the acetylcholine receptor pore. *Nature*, **423**, 949–955.
42. Beatty, K.E., Xie, F., Wang, Q., and Tirrell, D.A. (2005) Selective dye-labeling of newly synthesized proteins in bacterial cells. *J. Am. Chem. Soc.*, **127**, 14150–14151.
43. Ulbrich, M.H., and Isacoff, E.Y. (2007) Subunit counting in membrane-bound proteins. *Nat. Methods*, **4**, 319–321.
44. Mecozzi, S., West, A.P., Jr., and Dougherty, D.A. (1996) Cation- $\pi$  interactions in aromatics of biological and medicinal interest: Electrostatic potential surfaces as a useful qualitative guide. *Proc. Natl. Acad. Sci. USA*, **93**, 10566–10571.
45. Rodriguez, E.A., Lester, H.A., and Dougherty, D.A. (2007) Improved amber and opal suppressor tRNAs for incorporation of unnatural amino acids *in vivo*. Part 1: Minimizing misacylation. *RNA*, **13**, 1703–1714.
46. Rodriguez, E.A., Lester, H.A., and Dougherty, D.A. (2007) Improved amber and opal suppressor tRNAs for incorporation of unnatural amino acids *in vivo*. Part 2: Evaluating suppression efficiency. *RNA*, **13**, 1715–1722.
47. Quick, M.W., and Lester, H.A. (1994) Methods for expression of excitability proteins in *Xenopus* oocytes. In Narahashi, T. (ed.), *Ion Channels of Excitable Cells*. Academic Press, San Diego, CA, Vol. 19, pp. 261–279.